A Direct Swing Constraint-based Trajectory Planning Method for Underactuated Overhead Cranes

WANG Peng-Cheng[1, 2]   FANG Yong-Chun[1, 2]   JIANG Zi-Ya[3]

Abstract This paper proposes a novel swing constraint-based trajectory planning method for nonlinear overhead crane systems. To enhance the efficiency and security of the transportation process, some desired trajectories are designed to achieve the following merits: 1) leading the trolley to reach the destination sufficiently fast; 2) keeping the payload swing in an acceptable domain; 3) eliminating the residue swing when the trolley stops at the desired position. Specifically, the trajectories are divided into three stages. For each stage, the desired curve of the swing angle is directly constructed in accordance with anti-swing and zero-residual swing requirements, based on which the trolley trajectory is then obtained by analyzing the nonlinear kinematics of the crane system. An optimization mechanism is introduced to make intelligent compromises among the indices of transportation time, maximal swing angle, and so on. Both simulation and experimental results are provided to demonstrate the performance of the proposed direct swing constraint-based trajectory planning method.

Key words Trajectory planning, overhead cranes, swing, optimization, nonlinear kinematics

Owing to the high transportation efficiency and great convenience, overhead cranes have been widely utilized in ports, product lines, and so on[1]. However, most of these systems in practice are manually operated by long-time training workers, which present such drawbacks as low efficiency, low security, and so on[2]. For this reason, some researchers have started to address the control problem for overhead cranes[3]. However, as a typical underactuated system, the trolley motion and payload swing, which are coupled with each other, can only be controlled by the trolley's pull force, which makes the crane control problem very challenging[4−5].

Recently, much effort has been put on the advanced control algorithm development for underactuated overhead cranes[6]. As a result, many ambitious control strategies have been designed to improve system performance in terms of both transportation efficiency and payload swing[7]. For example, by convolving the operational signal with some impulse series, the input shaping techniques were implemented successfully[8−9]. Besides open-loop control methods, some kinds of closed-loop control strategies have also been proposed[10]. For example, Ma et al. designed a series of energy based controllers to drive the trolley to a desired position, and eliminate the payload swing efficiently[11−12].

As supported by much operation experience, the trajectory of the trolley plays a very important role for the efficiency and security of the transportation task. For the motion planning problem of overhead cranes, the designed trolley trajectory needs to satisfy the following requirements: there is no residue swing at the end of transportation; the trolley arrives at the destination fast enough; the swing is kept in an acceptable range during the overall process. Unfortunately, due to the underactuated character-

istics of the cranes, these requirements are usually incompatible with each other. For example, high transportation efficiency involves a large trolley velocity and acceleration, which usually tends to cause a large swing angle. Therefore, the desired trajectories need to make compromises between these indices. Additionally, when planning trajectories, practical conditions, such as the constraints on the magnitudes/directions of velocity and acceleration of the cart, need to be taken into account carefully to make the constructed trajectory trackable. Consequently, some optimization algorithm is introduced to generate the trajectories for the trolley which regulate the payload swing promptly. Additionally, some kinds of path planner, along with tracking controllers, are also invited for underactuated overhead cranes[13−14].

Though the trajectory planning problem of overhead cranes has attracted considerable attention[15], it needs to point out that the existing results are usually based on the linearized model and they can not tackle the aforementioned indices efficiently. In this research, a novel motion planning strategy directly based on the requirements of the payload swing is designed to enhance the operation performance. Specifically, based on the nonlinear model of an overhead crane, the swing trajectory of the payload is selected to meet the requirements of fast transportation and zero residual swing, with the impact of cable length variation fully considered. Based on the swing curve of the payload, the nonlinear model of overhead cranes is then employed to calculate the trajectory of the cart. To increase the flexibility of the trajectories, some optimization function is defined to intelligently tune the parameters of the trajectory to meet the requirements for different transportation tasks, and the powerful particle swarm optimization algorithm (PSO) is utilized to solve this nonlinear optimization problem with practical constraints. Compared with currently available methods, the proposed trajectory planning method presents the following two merits: firstly, it generates an ideal trajectory based on the accurate nonlinear model without any approximation; secondly, by directly considering the constraints on the payload swing, it constructs the swing profile of the payload, based on which the trajectory of the cart is then calculated by utilizing the kinematics of the studied crane system.

The rest of the paper is organized in the following man-

ner. In Section 1, a kinematic model of a 2-dimensional overhead crane system is introduced. Section 2 proposes the direct swing constraint-based trajectory planning method, including the steps of depicting the curves' shape, describing the optimization problem theoretically and utilizing the PSO algorithm to obtain the solution efficiently. Section 3 provides some simulation and experimental results to demonstrate the performance of the proposed trajectory planning method. And Section 4 provides the conclusions of the paper.

1   System model

In this section, a kinematic model of an overhead crane is depicted, which demonstrates how the payload swing is induced by the trolley's motion and payload lifting operation. For the trajectory planning task, we need to construct a superior trajectory for the trolley which satisfies physical constraints and achieves ideal indices, instead of designing a controller to drive the trolley to the desired location. Therefore, when analyzing the system model, we mainly focus on the kinematic characteristics, but not the dynamics relating the actuating force to the motion of the system.
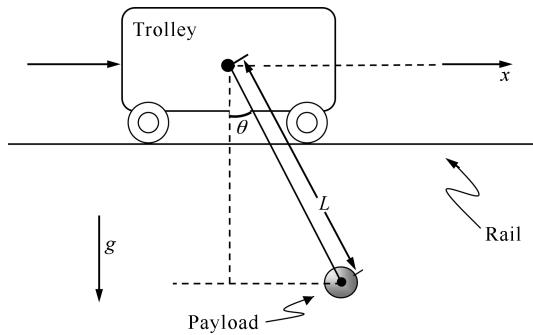

Fig. 1   A 2-dimensional overhead crane system

Considering the 2-dimensional overhead crane shown in Fig. 1, we can acquire the following kinematic model[16], whose correctness has been experimentally proven:

$$\cos\theta \ddot{x} + L\ddot{\theta} + 2\dot{\theta}\dot{L} + g\sin\theta = 0 \qquad (1)$$

where $x(t)$, $L(t)$ and $\theta(t)$ are the degrees of freedom of the crane system, which stand for the trolley position, the cable length and the payload's swing angle, respectively. The constant parameter g is the gravity acceleration. When the cable length is constant, (1) can be simplified to

$$\cos\theta \ddot{x} + L\ddot{\theta} + g\sin\theta = 0 \qquad (2)$$

Remark 1. The air friction of the payload is neglected in the model (1) due to the following reasons: the friction impact in this kinematic equation is dominated by the shape, size and mass of the payload, and the payload-air relative velocity is not only influenced by the motion of the crane systems, but also influenced by the wind condition. Thus, this kind of impact is time-varying, uncertain and complex, which should be excluded in the motion planning task reasonably, but be addressed as uncertain disturbance conveniently when constructing the tracking controllers.

2   Swing constraint-based planning method

In practical operations, the overall trolley motion trajectory can be generally divided into three stages: acceleration stage, constant velocity stage and deceleration stage. In the first stage, the trolley starts to move with its velocity increasing continuously, until it reaches the maximum, and the system then enters the second stage. In which, the trolley keeps moving with the maximum velocity to the desired position. At last, the trolley decelerates so that it stops at the destination in the third stage. There are two different kinds of transportation process. In the first type, the transportation task is divided into three steps, with the first step lifting the cargo, the second step horizontally moving the cargo to the desired location, and the third one lowering the cargo to the ground. Fig. 2 demonstrates the moving process of step two, where there is no lifting or lowering involved and thus the cable length is kept constant. For the second type of transportation, to improve the efficiency, the lifting or lowering operation is implemented simultaneously with the horizontal moving, as usually in the first and third stages, respectively. Therefore, for this type of transportation process, as shown in Fig. 3, the cable is shortened in the first stage to lift the cargo, and lengthened in the third stage to lower it.
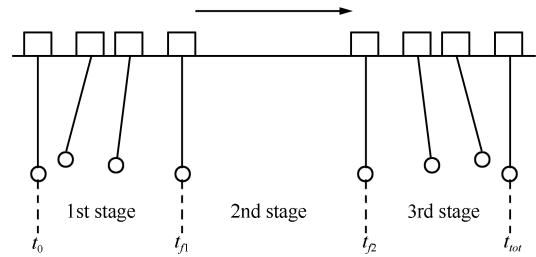

Fig. 2   Transportation without lifting/lowering operation
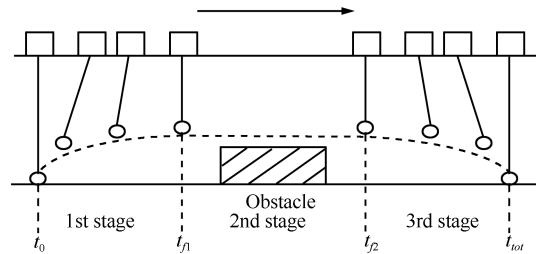

Fig. 3   Transportation with lifting/lowering operation

Our planning strategy also follows these basic principles. Therefore, the overall trajectory of the trolley motion $x(t)$ can be expressed as follows

$$x(t) = \begin{cases} x_1(t), & t \in [t_0, t_{f1}] \\ x_2(t), & t \in (t_{f1}, t_{f2}) \\ x_3(t), & t \in [t_{f2}, t_{tot}] \end{cases} \qquad (3)$$

and the swing angle curve $\theta(t)$ is

$$\theta(t) = \begin{cases} \theta_1(t), & t \in [t_0, t_{f1}] \\ \theta_2(t), & t \in (t_{f1}, t_{f2}) \\ \theta_3(t), & t \in [t_{f2}, t_{tot}] \end{cases} \qquad (4)$$

That is, the trolley starts to move at x_0, and reaches the desired position x_{tot} at t_{tot}. The curves $x_1(t)$ and $\theta_1(t)$ belong to the first stage of the acceleration stage $[t_0, t_{f1}]$. And the pairs of $(x_2(t), \theta_2(t))$ and $(x_3(t), \theta_3(t))$ are the trajectories of the second stage (t_{f1}, t_{f2}) and the third one $[t_{f2}, t_{tot}]$, respectively.

Ideally, the designed trajectories of $x(t)$ and $\theta(t)$ exhibit high transportation efficiency and lead to small payload

swing. At the same time, they satisfy the following constraints which are implied by the aim of zero-residual swing and the practical constraints of an overhead crane:

$$|\dot{x}(t)|_{\max} < V_{\max}, t \in [t_0, t_{tot}] \tag{5}$$

$$x(t_0) = x_0, x(t_{tot}) = x_{tot}, \dot{x}(t_0) = 0, \dot{x}(t_{tot}) = 0 \tag{6}$$

$$\dot{x}(t) = \dot{x}(t_{f1}), t \in [t_{f1}, t_{f2}] \tag{7}$$

$$\ddot{x}(t_{f1}) = 0, \ddot{x}(t_{f2}) = 0, \ddot{x}(t_{tot}) = 0 \tag{8}$$

$$\ddot{x}(t) > 0, t \in (t_0, t_{f1}), \ddot{x}(t) < 0, t \in (t_{f2}, t_{tot}) \tag{9}$$

$$\theta(t_0) = \theta(t_{f1}) = \theta(t_{f2}) = \theta(t_{tot}) = 0 \tag{10}$$

$$\dot{\theta}(t_0) = \dot{\theta}(t_{f1}) = \dot{\theta}(t_{f2}) = \dot{\theta}(t_{tot}) = 0 \tag{11}$$

$$\ddot{\theta}(t_0) = \ddot{\theta}(t_{f1}) = \ddot{\theta}(t_{f2}) = \ddot{\theta}(t_{tot}) = 0 \tag{12}$$

Apparently, $(10) \sim (12)$ guarantee the constraint on the payload swing, and constraints $(5) \sim (9)$ are imposed to ensure identical pull directions at each stage, aiming to make the curve much easier to track, and to satisfy some practical conditions.

Subsequently, the desired trajectories need to be constructed explicitly to satisfy the previous constraints $(5) \sim (12)$. That is, we need to design suitable functions for all the stages to meet the imposed requirements. To this end, some mathematical analysis for the three different stages of the desired trajectory is implemented to facilitate the subsequent planning. Though the subsequent analysis only focuses on the transportation process, the designed strategy can be easily combined with lifting/lowering operation to tackle more general operations.

The first stage. The task in this stage is to determine the trajectories of trolley movement and payload swing to meet the physical requirements. To this end, we directly choose function $\theta_1(t)$ of the payload swing, with the aim of keeping the swing angle in some acceptable domain and achieving zero-residual swing performance at the end of this stage, then the kinematics (2) is utilized to compute the cart movement $x_1(t)$ in the first stage.

From constraints of $(10) \sim (12)$, we know that function $\theta_1(t)$ has zeros of third order at time t_0 and time t_{f1}. Based on this fact, and to simplify the path planner, the curve of $\theta_1(t)$ is taken as the following polynomial function:

$$\theta_1(t) = -k_0(t - t_0)^3(t - t_{f1})^3 \tag{13}$$

where k_0 is a positive constant. By calculating the peek of the polynomial, the maximal swing angle $|\theta|_{\max}$ can be obtained from the previous formula as

$$|\theta|_{\max} = \frac{k_0(t_{f1} - t_0)^6}{64} \tag{14}$$

at the time of

$$t_{\max} = \frac{t_0 + t_{f1}}{2} \tag{15}$$

For an overhead crane system, the payload swing is usually much less than $\pi/2$, therefore, the kinematics (2) can be re-written into the following manner

$$\ddot{x} = \frac{-L\ddot{\theta} - g\sin\theta}{\cos\theta} \tag{16}$$

Subsequently, the cart movement in the first stage $x_1(t)$ can be calculated as

$$x_1(t) = x_1(t_0) + \iint_t \frac{-L\ddot{\theta}(t) - g\sin\theta(t)}{\cos\theta(t)}(\mathrm{d}t)^2, t \in [t_0, t_{f1}] \tag{17}$$

The second stage. Clearly, since the trolley moves uniformly in this stage, its position $x_2(t)$ can be calculated from the first stage $x_1(t)$ as

$$x_2(t) = \dot{x}_1(t_{f1})(t - t_{f1}) + x_1(t_{f1}), t_{f1} \leq t \leq t_{f2} \tag{18}$$

Meanwhile, during the second stage, we have $\ddot{x}(t) = 0$; substituting this fact into model (2) yields

$$L\ddot{\theta} + g\sin\theta = 0 \tag{19}$$

This formula, together with the constraint of $\theta(t_{f1}) = 0$, directly implies that in the second stage

$$\theta_2(t) = 0 \tag{20}$$

Equations (18) and (20) consist of the trajectories for the second stage.

The third stage. After noting the fact that the third stage and the first stage are symmetric (please see Figs. 2 and 3), we will try to calculate the curves of the third stage based on the functions of the first stage. As clearly shown in Figs. 2 and 3, the acceleration and deceleration operations, which correspond to the first and the third stages, are inverse processes. Based on the symmetric property of the velocity curve, it can be shown that

$$\dot{x}_3(t) = \dot{x}_1(t_{f1} + t_{f2} - t), t \in [t_{f2}, t_{tot}] \tag{21}$$

After some mathematical calculation, it can be shown that the trolley position in the third stage $x_3(t)$ is related to the first two stages of $x_1(t)$ and $x_2(t)$ in the following manner

$$x_3(t) = x_1(t_{f1}) + x_2(t_{f2}) - x_1(t_{f1} + t_{f2} - t), t \in [t_{f2}, t_{tot}] \tag{22}$$

Also, from the symmetric property of the desired trajectory, it can be seen that in the third stage, the payload swings in a similar manner as in the first stage. Yet, since the excitation $\ddot{x}_3(t)$ is in the opposite way of $\ddot{x}_1(t)$, from model (2), we know that

$$\theta_3(t) = -\theta_1(t_{f1} + t_{f2} - t) \tag{23}$$

Lifting/lowering operation. If lifting/lowering operation is required during transportation, the trajectories of cable length $L_1(t), L_2(t)$, and $L_3(t)$ are designed for the heaving, forwarding and lowering stages, respectively. As shown in Fig. 3, the first and third stages correspond to the lifting and lowering processes, respectively. For the sake of simplicity, the variation of the cable length is selected to take some polynomial form so as to obtain sufficiently smooth velocities and accelerations between zero and the maximum value. Yet, other selections for the change of the cable length can possibly exhibit the same characteristics, but with more complex calculation. In details, let L_0 and L_f be the initial and desired cable lengths, respectively. Then the length's curve of the first stage can be chosen as

$$L_1(t) = L_0 + (t - t_0)^3 \left[a(t - t_0)^2 + b(t - t_0) + c \right] \tag{24}$$

where $t \in [t_0, t_{f1}]$, and to ensure the smooth condition, constants a, b, and c in (24) are selected as follows

$$a = \frac{6(L_f - L_0)}{(t_{f1} - t_0)^5}, b = -\frac{15(L_f - L_0)}{(t_{f1} - t_0)^4}, c = \frac{10(L_f - L_0)}{(t_{f1} - t_0)^3}$$

Clearly, from the overhead crane operation requirements (please refer to Fig. 3), we know that in the second stage, the cable length will be kept constant as

$$L_2(t) = L_f \tag{25}$$

and the cable length in the third stage takes a symmetric form of $L_1(t)$ in the sense that

$$L_3(t) = L_1(t_{f1} + t_{f2} - t), t \in [t_{f2}, t_{tot}] \quad (26)$$

Optimization. For a transportation task, given the distance between the initial position x_0 and the desired position x_{tot}, together with the initial and desired cable lengths, the aim is to tune parameters t_{f1} and k_0 to make both the maximal swing $|\theta|_{\max}$ and the transportation time $\Delta t = t_{tot} - t_0$ as small as possible, where $|\theta|_{\max}$ is depicted in (14), and Δt can be calculated by summating the time for the three stages (see Figs. 2 and 3)

$$\Delta t = 2 (t_{f1} - t_0) + \frac{x(t_{f2}) - x(t_{f1})}{\dot{x}(t_{f1})} \quad (27)$$

where the symmetric property of the first and the third stages is utilized. Besides, $x(t_{f2})$ can be calculated as

$$x(t_{f2}) = x_{tot} - [x(t_{f1}) - x_0] = x_{tot} + x_0 - x(t_{f1}) \quad (28)$$

After substituting (28) into (27), the transportation time Δt can be finally obtained as

$$\Delta t = 2 (t_{f1} - t_0) + \frac{x_{tot} + x_0 - 2x(t_{f1})}{\dot{x}(t_{f1})} \quad (29)$$

Obviously, the motion planning strategy has to keep balance between the two indices $|\theta|_{\max}$ and Δt. That is, the shorter Δt, the larger acceleration of the cart, and subsequently the larger swing $|\theta|_{\max}$. Therefore, to make suitable compromises with the constraints, the following optimization function $F_{((t_{f1}-t_0),k_0)}$ is introduced

$$F_{((t_{f1}-t_0),k_0)} = \Delta t + \alpha |\theta|_{\max} \quad (30)$$

where constant $\alpha > 0$ is an empirical weighting factor varying for different operations.

To find the solution $((t_{f1} - t_0), k_0)$ for this multi-variable nonlinear optimization problem, the PSO technique is utilized[17]. The process of this algorithm is depicted as follows:

Step 1. Initialize particles and determine the maximal number of iterations. In this problem, the position of every particle is set as $((t_{f1} - t_0), k_0)$.

Step 2. Calculate the value of the optimization function $F_{((t_{f1}-t_0),k_0)}$. Testify whether the set of particles satisfies the constraints. If not, remove it and initialize another one.

Step 3. For every particle, compare its current value with its best one in history, and update its position $((t_{f1} - t_0), k_0)$.

Step 4. For every particle, compare the value with the best one in the swarm.

Step 5. Update the particle's velocity and position. Specifically, the moving velocity vector of the i-th particle x_i in the d-th dimension v_i^d is renewed as

$$v_i^d = w v_i^d + c_i r_1 \left(p_i^d - x_i^d\right) + c_i r_2 \left(p_g^d - x_i^d\right) \quad (31)$$

and its new position can be obtained as

$$x_i^d = x_i^d + v_i^d \quad (32)$$

where $i = 1, \cdots, m$ is the index number, p_i^d is the current best value of the i-th particle in the d-th dimension, p_g^d is the current best value of the whole group. And w, c_1 and c_2 are constants, while $r_1, r_2 \in (0, 1)$ are random numbers.

Step 6. Return to Step 2 until the process reaches the maximal number of iterations.

Remark 2. Different from the existing methods, the proposed trajectory planner directly selects the payload swing curve from the system requirements. The choice of function $\theta_1(t)$ is not unique, and it determines all of the other curves. Therefore, it plays the most important role for the considered path planning problem. In this research, function $\theta_1(t)$ is chosen as a polynomial, whose validity will be supported by the subsequent experimental results.

3   Simulation and experiments

To illustrate the performance of the proposed direct swing constraint-based trajectory planner, the constructed trajectories are first tested in Matlab/Simulink environment. And then some experiments on a crane testbed are further conducted to provide more convincing results. Considering that the work is on a motion planning task, to observe the performance of the constructed trajectories, a proportional-derivative (PD) controller is utilized in the experiments to enable the trolley to track the desired trajectories[1]. Please note that it is a general practice to check the performance of a trajectory planner with a conventional tracking controller[15−16].

For the simulation, the parameters for the transportation operation are selected as follows:

$$x_0 = 0 \, \text{m}, x_{tot} = 10 \, \text{m}, L_0 = 3 \, \text{m}, L_f = 1.5 \, \text{m}$$

with the maximum velocity chosen as

$$V_{\max} = 1.5 \, \text{m/s}$$

After the optimization process based on the PSO algorithm, the important parameters are determined as

$$\Delta t = 3.07, k_0 = 0.084$$

and function $F(\Delta t, k_0)$ with $\alpha = 25$ reaches the minimum of 12.31. For the proposed trajectory planning algorithm, the corresponding equations can be employed to calculate the parameters as follows:

$$t_0 = 0, t_{f1} = 3.07, t_{f2} = 6.50, t_{tot} = 9.57,$$
$$\Delta t = 9.57 \, \text{s}, |\theta|_{\max} = 0.11 \, \text{rad}$$

From the simulation results (Figs. 4 and 5), it can be seen that the trajectories satisfy the constraints in the overall process and the payload reaches the destination without any residue swing.
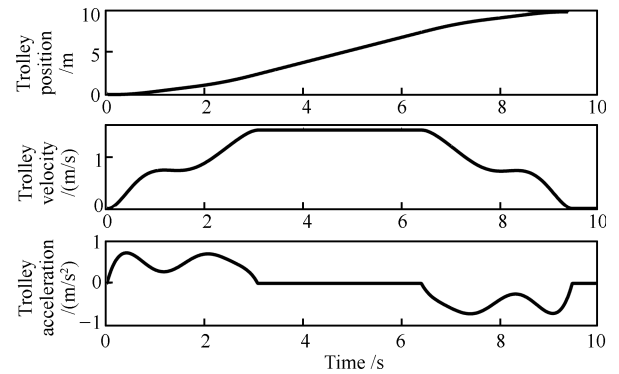

Fig. 4   The trolley motion trajectories

---

[1]A PD controller is very popular in industrial systems, it is thus adopted in the experiments as the tracking controller.
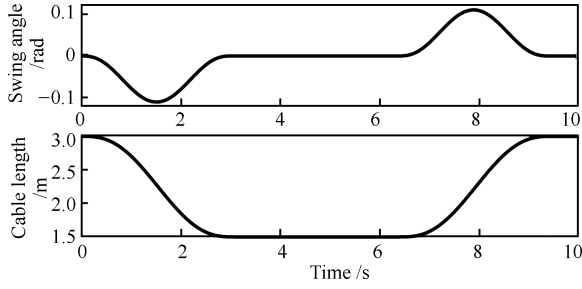
Fig. 5 The swing angle and cable length trajectories

To test the effect of the method in practical conditions, the planned trajectory $x(t)$ is employed in a scaled crane system[18] as the desired trajectory, and the PD controller is adopted to drive the trolley to track the curve $x(t)$

$$F_C(t) = ke_p(t) + k_d\dot{e}_p(t) \tag{33}$$

where k_p, k_d are positive, constant control gains, $e_p(t)$ represents the trolley tracking error

$$e_p(t) = x_p(t) - x(t)$$

with $x_p(t)$ denoting the desired trolley position, and $x(t)$ standing for its actual position which can be detected by on-board encoders.

Considering the actual size of the crane testbed, we determine the parameters for the transportation task as

$$x_0 = 0\,\mathrm{m}, x_{tot} = 0.6\,\mathrm{m}, L = 0.4\,\mathrm{m}$$

and the permitted maximum trolley velocity is

$$V_{\max} = 0.3\,\mathrm{m/s}$$

After the optimization process, the parameters are

$$\Delta t = 1.05, k_0 = 4.2237$$

and function $F(\Delta t, k_0)$ with $\alpha = 5$ reaches the minimum. Besides, the other parameters are calculated as

$$t_0 = 0, t_{f1} = 1.005, t_{f2} = 1.955, t_{tot} = 2.960$$
$$\Delta t = 2.960\,\mathrm{s}, |\theta|_{\max} = 0.068\,\mathrm{rad}$$

For the PD controller, the control gains are sufficiently tuned to achieve the best performance, which yields

$$k_p = 700, k_d = 200$$

The experimental results are shown in Figs. 6 and 7, which depict the tracking performance for the trolley position and the payload swing, respectively. From these results, we can conclude that the planned trajectories, even when combined with the conventional PD controller, can achieve satisfactory performance. From Fig. 6, it can be seen that the PD controller drives the trolley to follow the planned trajectory very closely, with the velocity under the permitted threshold. Please note that the tracking errors at the starting/ending points of different stages are mainly caused by the flaw of the mechanical and servo systems. As can be seen from Fig. 7, the payload swings closely to the planned functions, though some time offset is observed in the curves. The maximum swing angle is less than 3.5 degrees and the residual swing is almost neglectable, which sufficiently demonstrates the superior performance of the proposed trajectory planning method.
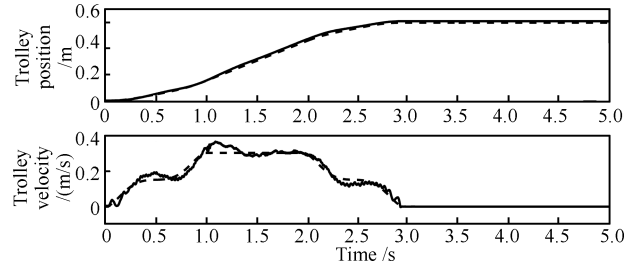

Fig. 6 Tracking results of the trolley position and velocity (The solid lines denote the tracking results, while the dash lines represent the desired trajectories.)
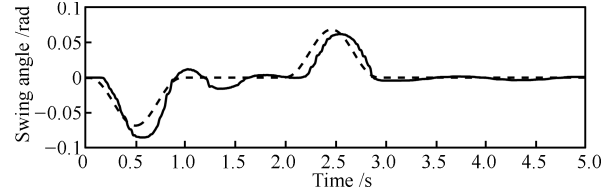

Fig. 7 Tracking results of the payload swing angle (The solid line denotes the tracking result while the dash line represents the desired trajectory.)

4 Conclusions

In this paper, a novel swing constraint-based trajectory planning method is designed for nonlinear overhead cranes, so as to improve the efficiency and security of the transportation process. Based on practical requirements of crane operations, the trajectories are divided into three stages. For each stage, the desired curve of the swing angle is directly designed from the indices of acceptable swing angle, zero-residual swing, and so on. And then, the trajectory of the trolley is calculated by analyzing the nonlinear kinematics model. An optimization mechanism is utilized to make an intelligent compromise among the indices of transportation time, maximal swing angle, and so on. The performance of the proposed swing constraint-based trajectory planning method is verified by both simulation and experimental results. Finding better forms of swing curves in the future work is critical for us to enforce the capacity of this novel trajectory planning method.

References

1 Ngo Q H. Adaptive sliding mode control of container cranes. *IET Control Theory and Applications*, 2012, **6**(5): 662−668

2 Sun N, Fang Y C. New energy analytical results for the regulation of underactuated overhead cranes: an end-effector motion based approach. *IEEE Transactions on Industrial Electronics*, 2012, **59**(12): 4723−4734

3 Peng K C C, Singhose W, Frakes D H. Hand-motion crane control using radio-frequency real-time location systems. *IEEE/ASME Transactions on Mechatronics*, 2012, **17**(3): 464−471

4 Sun N, Fang Y C, Zhang X B. An increased coupling-based control method for underactuated crane systems: theoretical design and experimental implementation. *Nonlinear Dynamics*, 2012, **70**(2): 1135−1146

5 Fang Y C, Wang P C, Sun N, Zhang Y C. Dynamics analysis and nonlinear control of an offshore boom crane. *IEEE Trans. on Industrial Electronics*, 2014, **61**(1): 414−427

6 Ngo Q H, Hong K S. Sliding-mode antisway control of an offshore container crane. *IEEE/ASME Transactions on Mechatronics*, 2012, **17**(2): 201−209

7 Zavari K, Pipeleers G, Swevers J. Gain-scheduled controller design: illustration on an overhead crane. *IEEE Transactions on Industrial Electronics*, 2014, **61**(7): 3713−3718

8 Garrido S, Abderrahim M, Giménez A, Diez R, Balaguer C. Anti-swinging input shaping control of an automatic construction crane. *IEEE Transactions on Automation Science and Engineering*, 2008, **5**(3): 549−557

9 Singhose W, Vaughan J. Reducing vibration by digital filtering and input shaping. *IEEE Transactions on Control Systems Technology*, 2011, **19**(6): 1410−1420

10 Park M, Chwa D, Hong S. Antisway tracking control of overhead cranes with system uncertainty and actuator nonlinearity using an adaptive fuzzy sliding-mode control. *IEEE Transactions on Industrial Electronics*, 2008, **55**(11): 3972−3984

11 Ma B, Fang Y, Zhang Y. Switching based emergency braking control for an overhead crane system. *IET Control Theory Application*, 2010, **4**(9): 1739−1747

12 Sun N, Fang Y C, Zhang X B. Energy coupling output feedback control of a 4-DOF underactuated crane with saturated inputs. *Automatica*, 2013, **49**(5): 1318−1325

13 Sun N, Fang Y C, Zhang Y D, Ma B J. A novel kinematic coupling based trajectory planning method for overhead cranes. *IEEE/ASME Transactions on Mechatronics*, 2012, **17**(1): 166−173

14 Yoshida K, Matsumoto I. Load transfer control for a crane with state constraints. In: Proceedings of the American Control Conference. St. Louis, MO, USA: IEEE, 2009. 2551−2557

15 Sun N, Fang Y C, Zhang X B, Yuan Y H. Transportation task-oriented trajectory planning for underactuated overhead cranes using geometric analysis. *IET Control Theory & Applications*, 2012, **6**(10): 1410−1423

16 Sun N, Fang Y C. An efficient online trajectory generating method for underactuated crane systems. *International Journal of Robust and Nonlinear Control*, 2014, **24**(11): 1653−1663

17 Ma G, Zhou W, Chang X L. A novel particle swarm optimization algorithm based on particle migration. *Applied Mathematics and Computation*, 2012, **218**(11): 6620−6626

18 Fang Y C, Ma B J, Wang P C, Zhang X B. A motion planning-based adaptive control method for an underactuated crane system. *IEEE Transactions on Control Systems Technology*, 2012, **20**(1): 241−248

WANG Peng-Cheng   Ph. D. candidate in the Mechanical and Aerospace Engineering Department, Rutgers University, USA. His research interest covers dynamics and control of underactuated overhead cranes, wheeled mobile robots and underwater autonomous glider.
E-mail: mechaerowpc@gmail.com

FANG Yong-Chun   Professor at the Institute of Robotics and Automatic Information System (IRAIS), Nankai University. His research interest covers visual servoing, control of underactuated systems including overhead cranes. Corresponding author of this paper.
E-mail: yfang@robot.nankai.edu.cn
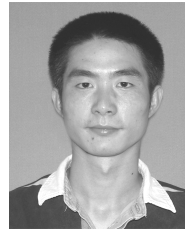
JIANG Zi-Ya   Ph. D. candidate at the State Key Laboratory of Robotics, Shenyang Institute of Automation, Chinese Academy of Sciences. His research interest covers dynamics and control of underactuated overhead cranes, disturbance estimation and attenuation of unmanned aerial vehicles.
E-mail: hbtmjzy@gmail.com